Flame inhibition by calcium compounds: Effects of calcium compounds on downward flame spread over solid cellulosic fuel

Yusuke Koshiba [a,*], Takuya Haga [b], Hideo Ohtani [c]

[a] Department of Materials Science and Chemical Engineering, Faculty of Engineering, Yokohama National University, 79-5 Tokiwadai, Hodogaya-ku, Yokohama 240-8501, Japan

[b] Graduate School of Environmental and Information Sciences, Yokohama National University, 79-7 Tokiwadai, Hodogaya-ku, Yokohama 240-8501, Japan

[c] Department of Safety Management, Faculty of Environmental and Information Sciences, Yokohama National University, 79-7 Tokiwadai, Hodogaya-ku, Yokohama 240-8501, Japan

* Corresponding author: Telephone number: +81 45 339 3985

Fax number: +81 45 339 3985

E-mail address: koshiba-yusuke-xm@ynu.ac.jp

Complete postal address: 79-5 Tokiwadai, Hodogaya-ku, Yokohama 240-8501, Japan

Abstract

Owing to depletion risks and the rising cost of phosphate rock, phosphorus-free fire-extinguishing agents are in growing demand. This paper aims to develop a new fire suppressant that does not use phosphates and reports the flame-inhibition properties of calcium compounds: calcium acetylacetonate ($Ca(acac)_2$), calcium acetate ($Ca(OAc)_2$), calcium hydroxide ($Ca(OH)_2$), calcium carbonate ($CaCO_3$), calcium nitrate ($Ca(NO_3)_2$), and calcium oxide (CaO). Their flame-inhibition capabilities were evaluated by measuring the downward flame-spread rates over cellulosic fuels on which each calcium compound was adsorbed. Suppression experiments demonstrated that $Ca(acac)_2$, $Ca(OAc)_2$, $Ca(OH)_2$, and $CaCO_3$ extinguished flames. $Ca(OAc)_2$ and $Ca(acac)_2$ were more effective by factors of approximately 1.6 and 1.4, respectively, than ammonium dihydrogen phosphate. To elucidate the influences of the calcium compounds on the pyrolysis of cellulose and char combustion, the activation energy (E) and pre-exponential factor (A) associated with the pyrolysis of cellulose and the char yield (Y) were determined by kinetic analyses involving thermogravimetric measurements. The kinetic analysis permitted us to conclude that none of the calcium compounds hindered cellulose pyrolysis or char combustion. A positive correlation between the bond energy of the compound and minimum extinction concentrations was found, thus suggesting that compounds that easily release atomic calcium effectively inhibit flames.

Keywords: Calcium compound, Combustion inhibition, Fire suppression, Minimum extinction concentration, Phosphorus free, Fire extinguishing agent

Abbreviations

A	Pre-exponential factor (min^{-1})
Ac	Acetyl
acac	Acetylacetonate
ADP	Ammonium dihydrogen phosphate
C_k	Concentration of compound k calculated from Eq. (2) (mol g^{-1}) on the rectangular paper specimen
C_E	Minimum extinction concentration (MEC, mol g^{-1})
c_p	Heat capacity of the solid fuel (J g^{-1} K^{-1})
DTG	First derivative of TG curve
E	Activation energy (kJ mol^{-1})
E_b	Bond energy (kJ mol^{-1})
g	Acceleration due to gravity (m^2 s^{-1})
M	Molar mass (g mol^{-1})
Me	Methyl

R	Gas constant (8.31 J mol^{-1} K^{-1})
R^2	Coefficient of determination (dimensionless)
r.t.	Room temperature
T	Temperature (K)
t	Time (min)
T_{max}	Temperature at which the weight-loss rate is the maximum (K)
TG	Thermogravimetry
U	Downward flame-spread rate (mm s^{-1})
V	Normalized downward flame-spread rate (dimensionless)
W	Weight (mg)
X	Third body
Y	Char yield (%)

Greek letters

β	Heating rate (K min^{-1})
δ	Solid-fuel thickness (m)
λ	Gas-phase thermal conductivity (W m^{-1} K^{-1})
ρ_s	Solid-fuel density (g m^{-3})

Subscripts

cel	Pure cellulose
f	Flame
g	Vaporization
k	Compound *k*
s	Specimen
∞	Ambient

1. Introduction

Powder fire extinguishers are used to contain and extinguish incipient fires in emergencies globally. Fire suppressants limit the spread of fires and mitigate losses of life and property. A typical effective component in dry-chemical extinguishers is ammonium dihydrogen phosphate (ADP, $NH_4H_2PO_4$). Unfortunately, phosphate-derived fire-extinguishing agents face serious limitations in today's market. A recent study warned that a future demand for phosphorus resource, which is also needed in agricultural fertilizers, will increase significantly [1]. Furthermore, phosphate rock is being traded at a high price [2] and is at high risk of depletion [3]. Hence, such a situation requires an alternative

phosphorus-free fire-extinguishing agent.

Thus far, several previous studies on phosphorus-free agents have been available in the literature [4–6]. For instance, Ni et al. [7] developed manganese compounds supported by zeolite particles and found that the powders had optimal values of transition-metal concentrations in terms of suppression efficiency. Koshiba et al. [8] reported that several chromium and manganese compounds exhibited more effective flame-inhibition ability than ADP. Chen et al. [9] experimentally demonstrated that $KHCO_3$–γ-Al_2O_3 composites had a higher extinguishing efficiency than ADP-based dry chemicals.

In contrast to alkali and rare-metal compounds, few studies on calcium compounds have been published notwithstanding their low risk of depletion and strong suppression ability. Cotton and Jenkins reported calcium-catalyzed radical recombination reactions [10], whereas Zalosh [11] and Fluegeman et al. [12], in investigating fire-extinguishing agents for Class D fires (i.e., metal fires), reported experimental observations of the high suppression capability of calcium carbonate ($CaCO_3$).

The main objective of the present study was to explore the flame inhibition efficiency of calcium compounds. In this study, six calcium compounds were examined, as described later. The anions of the calcium compounds tested have little flame-inhibition ability, thus allowing us to eliminate the influence of the anions on their suppression efficiencies. The fire suppression ability of gaseous agents is generally assessed by measuring the burning velocity and extinction concentration using a burner (Mache–Hebra nozzle burner) and the total-area/angle method, whereas the efficiency of powdered

agents is generally evaluated using a cup burner [13]. However, one of the drawbacks of the cup-burner method is that it often requires relatively large amounts of suppressants to conduct suppression trials. In this work, combustion inhibition efficiency of calcium compounds was evaluated by measuring the downward flame spread rates over a thermally thin cellulosic fuel on which each suppressant was adsorbed. The method allows a direct comparison of the chemical inhibition efficiency of calcium compounds, as will be described in detail hereinafter.

2. Chemicals and materials

In this study, calcium acetylacetonate ($Ca(acac)_2$, > 98.0%), calcium acetate ($Ca(OAc)_2$, > 98.0%), calcium hydroxide ($Ca(OH)_2$, > 98.0%), $CaCO_3$ (> 99.5%), calcium nitrate ($Ca(NO_3)_2$, > 98.0%), and calcium oxide (CaO, > 97.0%) were used without further purification. The chemical structure of $Ca(acac)_2$ is shown in Fig. 1; the rest of the compounds is generally known.

Water to dissolve the powders was deionized to a conductivity of <1 μS cm^{-1}. Hardened filter papers, which consisted of >99% cellulose, with a density of 96 g m^{-2}, a uniform thickness of 0.12 mm, and an ash content of 0.025% [14] were employed in this work.

3. Measurements of downward flame spread rates: Determination of flame inhibition ability

3.1. Downward flame-spread rates over solid fuels

In this study, the flame-inhibition ability of the tested calcium compounds was experimentally determined by measuring the downward flame-spread rates over a thermally thin cellulosic fuel bed (i.e., filter paper) on which each compound was uniformly adsorbed. Cellulose is a typical solid fuel used for such tests.

Compared with thermally thick solid fuels, the thermal conduction via the solid fuel is generally negligible for thermally thin fuels [15]. In upward flame propagation, buoyant convection, diffusive transport, and flame spread are simultaneous and result in unsteady flame propagation [16]; whereas, in downward flame propagation, the spread rate and flame structure are quite steady [17]. Furthermore, an earlier experimental study by Ronney et al. [16] revealed that the downward flame spread rate, U, is more reproducible than the upward flame spread rate. For thermally thin fuels, the downward flame spread generally achieves a steady rate, and the rate can be expressed by the de Ris equation (Eq. (1), [18, 19]):

$$\boldsymbol{U = \frac{\sqrt{2}\lambda}{\rho_s c_p \delta}\left(\frac{T_f - T_g}{T_g - T_\infty}\right)}, \tag{1}$$

where λ is the gas-phase thermal conductivity, ρ_s is the solid-fuel density, c_p is the heat capacity of the solid fuel, δ is the solid-fuel thickness, T_f is the flame temperature, T_g is the vaporization temperature, and T_∞ is the ambient temperature. As described above, the paper specimens used in this study were sufficiently thermally thin. Eq. (1) shows that for the downward flame spread rate of cellulosic fuels, the flame spread rate is negatively correlated with the reciprocal of the thickness when $\delta < 15$ mm, i.e., $U \sim \delta^{-1}$; by contrast, in cases in which $\delta > 15$ mm, this relationship does not hold true because the sample is thermally thick, thus resulting in an unstable flame spread [20]. As pointed out by Drysdale [20], the shape (e.g., width) of a thermally-thin solid fuel influences the upward flame spread rate (i.e., flame spread rate ~ width$^{1/2}$), although the width has little effects on the downward flame spread rate.

As described later, the calcium compounds exerted a limited effect on the variables in Eq. (1), except for T_f, owing to low concentrations of the calcium compounds adsorbed on the filter papers. As reported by Bhattacharjee et al. [21], the flame-spread rates also vary depending on the ambient gas composition (e.g., oxygen concentration), gas flow velocity, ambient pressure, and gravity. For thermally thin fuels, Ronney et al. pointed out that the gas-flow velocity had little influence on the flame spread rate [16]. As will be noted later, all four variables were kept constant. Hence, the filter-paper combustion experiments allowed us to directly chemically compare the flame inhibition efficiency among the calcium compounds [22].

3.2. Specimen-preparation methods

The filter paper was cut into rectangular pieces (120.0-mm long × 5-mm wide) using teflon-coated scissors so as not to contaminate the paper specimens with trace amounts of metal powder. The rectangular paper was dried in a vacuum desiccator for at least 24 h and then weighed. The water-soluble compounds (calcium acetate and calcium nitrate) were dissolved in deionized water. The water-insoluble compounds, namely, calcium hydroxide, calcium oxide, and calcium carbonate, were finely ground and then dispersed in dry ethanol using sonication (43 kHz), whereas calcium acetylacetonate was thoroughly dissolved in tetrahydrofuran (dehydrated, > 99.5%). The dry rectangular papers were then immersed in each solution/dispersion for several minutes. The paper was dried thoroughly again in a vacuum desiccator and then weighed. The paper-specimens were laid down on an accordion-like jig to reduce the contact points between the paper-specimens and jig. Such procedure helped to prepare the specimens on which each compound was homogeneously adsorbed. Unfortunately, the sizes of the calcium compounds on the paper-specimens were too small to view them with the help of a FE-SEM (field emission scanning electron microscopy). Fig. 2 illustrates the specimen-preparation procedures.

The concentration of the adsorbed compound per unit weight of the rectangular paper was defined by the following equation:

$$C_{\mathrm{k}} = \frac{\left(\frac{W_{\mathrm{s}}}{W_{\mathrm{cel}}} - 1\right)}{M_{\mathrm{k}}}, \qquad (2)$$

where C_k is the concentration of the compound k on the rectangular specimen, W_{cel} represents the weight of the dry pure dry rectangular paper, W_s is the weight of the paper specimen on which each compound was homogeneously adsorbed, and M_k denotes the molar mass of compound k. Since filter papers have a porous structure, we were unable to simply calculate the actual volume and surface area of the filter-paper sample. Thus, we used the C_k value calculated from weight because of its easy evaluation.

3.3. Experimental procedures

The experimental apparatus we used for the suppression trials is shown in Fig. 3. Dry air was passed upward at a flow rate of 5.0×10^{-3} m^3 min^{-1} via a mass-flow controller and we verified that the air flow was laminar. Each specimen, which was fixed using a specimen holder in a tube (300-mm high × 80-mm diameter), was ignited at its upper edge using a small pilot flame (i.e., portable cigarette lighter). To eliminate the effect of the pilot flame, the downward flame spread rate was calculated by measuring the time during which the flame edge propagated from a point 10 mm below the top of the

sample to a point 70 mm below the top. The normalized downward flame spread rate V_k is given by

$$\boldsymbol{V_k = \frac{U_k}{U_{cel}}}, \quad (3)$$

where U_k is the flame spread rate of the specimen where compound *k* was adsorbed, and U_{cel} denotes the spread rate of a pure rectangular paper.

The reasonability of the filter-paper combustion test used in this study is discussed here. Several related researchers have employed the solid fuel combustion method for evaluating the flame inhibition efficiency. For instance, Feilchenfeld et al. [23] reported the flame spread rates of a solid fuel bed (polyester) impregnated with halides. McCater [24], in studying the combustion inhibition of undyed terry cloth that consisted of pure cellulose (ash content: ~ 0.10 wt%), measured the downward flame spread rates with and without 184 inorganic compounds and Koshiba et al. [22] evaluated the flame spread rates over cellulosic solid fuels on which metallocenes were adsorbed. Note that these suppression tests differ somewhat from the standard tests. Izumikawa et al. [25] pointed out that if a flame inhibitor influenced the pyrolysis/degradation reactions of solid fuel, the efficiency of the flame inhibitor that is adsorbed on a solid fuel would differ from that of an inhibitor that is discharged onto the combusting fuel. However, as stated later in Section 3.5, the calcium compounds have no effect on the degradation reactions of cellulose, assisting in validating the reasonability of the test.

3.4. Flame-inhibition mechanisms

The schematic models of the flame-inhibition mechanisms using the calcium compounds are shown in Fig. 4. Cotton and Jenkins, in discussing the calcium-catalyzed radical recombination reactions in flames, found that $Ca(OH)_2$, CaOH, and CaO act as major flame-inhibiting species [10].

In the flame-spreading process, the heat transfer from the flame to the unburned solid cellulosic fuel (i.e., filter-paper specimen) in the preheated zone pyrolytically yields volatile flammable vapors and leads to the formation of a diffusion flame [26]. To continue the production of fuel vapors and the self-sustaining combustion process, sufficient heat must be fed back to the fuel bed [27]. Together with the flammable vapors, the inhibitor vapor (or inhibitor-derived vapors, namely, inhibiting species) is produced simultaneously. At the top of the specimen, residual char burnout (i.e., combustion of char) occurs (Fig. 5).

If the inhibitor exhibits flame-inhibition ability in the gas phase, an increase in the inhibitor concentration on the cellulosic fuel (i.e., filter paper) gradually decreases the downward flame spread rate U, which eventually reaches zero (i.e., flame extinction). In cases in which the calcium compounds behave as flame inhibitors in the condensed phase, they hinder the decomposition of the cellulosic fuel itself and/or the burnout of the residual char, thus indicating that the inhibitor impedes the production

of volatile flammable vapors, eventually leading to the reduction of the flame-spread rate [22].

3.5. Results of the suppression experiments

The relationship between the normalized flame-spread rates and calcium-compound concentrations is shown in Fig. 6b–g. For reference, Fig. 6a shows the normalized flame spread rates as a function of ADP concentration. For all the samples, we verified that in the tests, (i) no glowing was observed in any of the specimens, (ii) the V values varied smoothly, and (iii) no re-ignition was observed when the concentration was greater than the corresponding minimum extinction concentration (MEC, C_E).

For $Ca(acac)_2$, $Ca(OAc)_2$, $Ca(OH)_2$, and $CaCO_3$, the flame spread rate decreased with increasing calcium concentration, eventually reaching $V = 0$, which indicates flame extinction. For the CaO specimen, the flame spread rate decreased gradually, as the calcium concentration increased. However, in the calcium concentration range of 0–2.22×10^{-3} mol g^{-1}, the flame spread rate approached a minimum value of $V = 0.85$ because of the adsorption limit of CaO on the rectangular filter paper. This study defined the adsorption limit at which each calcium-compound mass on the rectangular paper specimen increased no longer. For the $Ca(NO_3)_2$ specimen, the flame-spread rate exhibited a distinct U-shaped curve, owing to its oxidative tendency. Calcium nitrate is known to act as an oxidizer [28]

that accelerates fuel combustion, thus causing an increase in the flame spread rate.

Table 1 lists the C_E values of the calcium compounds that extinguished the filter-paper flame, along with the C_E value for ADP ($C_{E,\ ADP} = 0.53 \times 10^{-3}$ mol g^{-1}) [8]. The list in the table shows that $CaCO_3$ and $Ca(OH)_2$ had larger C_E values than ADP, which is a conventional fire-extinguishing agent. By contrast, the C_E values of $Ca(acac)_2$ and $Ca(OAc)_2$ were 0.36×10^{-3} and 0.31×10^{-3} mol g^{-1}, respectively. The C_E values of $Ca(acac)_2$ and $Ca(OAc)_2$ were reduced by a factor of approximately 1.4 and 1.6, respectively, compared with that of ADP. This result clearly shows that $Ca(acac)_2$ and $Ca(OAc)_2$ exhibited a significantly higher combustion inhibition ability than ADP.

4. Thermogravimetric analysis

Obtaining a clear insight into the phase is of paramount importance to understand the combustion-inhibition mechanisms. However, the flame spread rate was reduced in cases in which the calcium compounds exhibited the flame-inhibition efficiency in gas and/or solid phases, as presented in Section 3.4. This result clearly indicates that the combustion test alone is insufficient to determine the phase in which the calcium compounds exhibit their flame inhibition effects [22].

For this purpose, we additionally conducted thermogravimetric (TG) analysis. In this study, the thermal decomposition and combustion of cellulose mixed with calcium compounds were investigated

using the TG method, which is a commonly used method in related research fields [27]. TG is a suitable technique involving the measurement of sample mass changes as a function of temperature to gain information on solid-phase chemical reactions. As described above, when both the solid- and gas-phase inhibition effects would be observed in the filter-paper fire tests, we cannot conclude the phase where the calcium compounds tested exert their suppression ability. However, when no solid-phase inhibition efficiency of the calcium compounds is observed notwithstanding their excellent suppression effects in the filter-paper fire trials, the calcium compounds exhibit their inhibition effects not in the solid phase but in the gas phase by a process of elimination. Cheng et al. [29] studied the pyrolysis and combustion reactions associated with cellulosic fuels with a focus on determining the kinetic parameters: the activation energy (E) and the pre-exponential factor (A). Koshiba et al. [22] investigated the abilities of suppressants to extinguish cellulosic-fuel fires by calculating the char yield (Y) and the activation energy and pre-exponential factor. In the current study, as presented in detail later, the condensed-phase inhibition ability of the calcium compounds was assessed by comparing these three parameters (E, A, and Y) of the cellulose mixed with calcium compounds with those of pure cellulose. Using the TG method, the calcium compounds that completely extinguished the combustion of the filter paper (Section 3.5) were investigated.

Provided that Eqs. (4) and (5) hold, the calcium compounds with the flame-extinction ability (Section 3.5) will act as flame inhibitors in the condensed phase. In addition, the calcium compounds

are also determined to possess inhibition ability from the observation that the char yields are significantly large—Eq. (6).

$$E_s > E_{cel} \quad (4)$$

$$A_s < A_{cel} \quad (5)$$

$$Y_s > Y_{cel} \ (\approx 0) \quad (6)$$

where subscripts s and cel denote the calcium compound/cellulose mixture and pure cellulose, respectively.

In contrast, if no significant differences in terms of activation energy, pre-exponential factor, or char yield between the calcium compound/cellulose and pure cellulose specimens were observed, the calcium compounds can be determined to behave as flame inhibitors in the gas phase alone. This result is attributed to the fact that the conditions—Eqs. (7)–(9)—clearly reflect that no calcium compounds hamper the pyrolysis and char combustion in the solid phase, but they are able to extinguish a filter-paper fire.

$$\boldsymbol{E_s \approx E_{cel}} \quad (7)$$

$$\boldsymbol{A_s \approx A_{cel}} \quad (8)$$

$$\boldsymbol{Y_s \approx Y_{cel} (\approx 0)} \quad (9)$$

4.1. Specimen-preparation for TG analysis

As pointed out by Kim et al. [30], the influence of the cellulose crystallite size on the activation energy associated with the cellulose decomposition is negligible. In contrast, the pre-exponential factor of solid-phase reactions generally depends on the particle size [31]. To avoid these influences, the tested calcium compounds were well milled and then mixed with cellulose powder (<20 μm). The concentration of each calcium compound was set to the corresponding C_E value listed in Table 1.

4.2. Experimental and kinetic analysis methods

The TG measurements of pure cellulose with and without calcium compounds were performed using a Shimadzu TG analyzer (TGA-50, Japan). Specimens of approximately 2 mg were loaded into

aluminum pans. We confirmed that no significant differences existed in the TG curves among the specimens in the aluminum and alumina pans. In the TG measurements, the heating rates ($\beta = dT/dt$) were 5, 10, 15, and 20 K min^{-1} in the temperature range from room temperature (r.t.) to 873 K.

To determine the activation energy and pre-exponential factor associated with cellulose decomposition, the Kissinger kinetic method [32] was used. For first-order reactions, the Kissinger equation is expressed as follows:

$$\ln\left(\frac{\beta}{T_{max}^2}\right) = -\frac{E}{RT_{max}} + \ln\left(\frac{AR}{E}\right) \quad (10)$$

where T_{max} and R denote the temperature at which the weight-loss rate is maximized and the gas constant, respectively. Eq. (10) indicates that the activation energy E and the pre-exponential factor A can be obtained from the slope of $\ln(\beta\, T_{max}^{-2})$ against T_{max}^{-1} and its intercept, respectively.

The detailed reaction mechanisms associated with the pyrolysis/degradation of cellulose remain a contentious issue [33]. However, in any case, the cellulose combustion processes involve two prominent steps. As described in Section 3.4, the first step corresponds to cellulose pyrolysis at a temperature of approximately 520 K, which is a pseudo-first-order reaction [34]. The second step is due to char combustion at a temperature of approximately 700 K [35]. For this reason, in all the TG measurements, dry nitrogen (>99.99%) was purged at a flow rate of 50 mL min^{-1} in the temperature

range of r.t.–673 K, whereas the TG curves were obtained under dry air atmosphere at a flow rate of 50 mL min^{-1} in the temperature range of 673–873 K. The char yield at 873 K (*Y*) was determined by subtracting the residual weights at 873 K of the pure calcium compounds from those for the cellulose–calcium compound specimens.

4.3. TG and kinetic analysis results

Fig. 7 depicts the weight-loss history of the samples examined in this study at a heating rate of 10 K min^{-1} under a nitrogen atmosphere. For the pure cellulose (Fig. 7a), the weight started to decrease at ca. 560 K and only one weight-loss stage, which is attributed to the pyrolysis of cellulose, was undeniably observed. As shown in Fig. 7d and e, a decrease in weight loss was observed for the $Ca(OH)_2$/cellulose and $CaCO_3$/cellulose samples. The TG and its first derivative TG (DTG) curve of the $Ca(acac)_2$/cellulose sample consisted of a three-step weight-loss process (Fig. 7b). The comparison of Fig. 7b with Fig. 7f (pure $Ca(acac)_2$) revealed that for the $Ca(acac)_2$/cellulose sample, the first step at ca. 320 K corresponds to the loss of H_2O, whereas the second weight loss between ca. 560 and 580 K is related to the degradation of $Ca(acac)_2$ itself. As can be clearly seen in Fig. 7b and Fig. 7f, no significant differences in the DTG peak due to the degradation of $Ca(acac)_2$ were found, thus indicating no interactions between $Ca(acac)_2$ and cellulose in the condensed phase. For the $Ca(OAc)_2$/cellulose

sample (Fig. 7c), the weight decreased gradually with an increase in temperature of up to ca. 580 K, and then decreased steeply at 580–650 K. The first weight-loss step at lower temperatures (Fig. 7c and g) is due to the loss of H_2O: $Ca(OAc)_2{\cdot}H_2O \rightarrow Ca(OAc)_2 + H_2O$ [36]. No weight losses were observed in the range of 560–640 K.

Table 2 clearly shows that in the T_{max} values of pure cellulose with and without calcium compounds, no significant differences in the T_{max} values were observed. The result provides indisputable evidence that the pyrolysis of cellulose underwent approximately the same mechanisms regardless of the presence or absence of calcium compounds, thus allowing us to directly compare the kinetic parameters.

Fig. 8 shows the variations in $\ln(\beta\, T_{max}^{-2})$ as a function of T_{max}^{-1} for the cellulose with and without the calcium-compound specimens. These plots are almost linear with satisfactory coefficients of determination (R^2): $R^2_{Ca(acac)2} = 0.99$, $R^2_{Ca(OAc)2} = 1.00$, $R^2_{Ca(OH)2} = 1.00$, and $R^2_{CaCO3} = 1.00$.

The summary of the apparent activation energy and pre-exponential factors of $Ca(acac)_2$/cellulose, $Ca(OAc)_2$/cellulose, $Ca(OH)_2$/cellulose, and $CaCO_3$/cellulose is provided in Table 3, together with the E and A of pure cellulose for reference. The activation energy values of $Ca(acac)_2$/cellulose, $Ca(OAc)_2$/cellulose, $Ca(OH)_2$/cellulose, $CaCO_3$/cellulose, and pure cellulose were determined to be 169, 162, 161, 175, and 171 kJ mol^{-1}, respectively. Undoubtedly, no significant differences were observed in terms of E values. Table 3 also lists the natural logarithms of the pre-exponential factors

of $Ca(acac)_2$/cellulose, $Ca(OAc)_2$/cellulose, $Ca(OH)_2$/cellulose, $CaCO_3$/cellulose, and pure cellulose, clearly indicating that no significant differences were observed in the pre-exponential factors. Thus, the TG measurements allowed us to conclude that the calcium compounds do not hamper the pyrolysis of cellulose.

Table 4 lists the char-yield results. We note that the average char yields were determined with three TG measurements per specimen. We obviously observe the following: (i) no significant differences in terms of char yields between the calcium compound/cellulose and pure cellulose, and (ii) low char yields (<5%) in all the tested specimens. As such, the char-yield measurements clearly confirmed that the calcium compounds (or calcium-derived compounds) do not hinder char combustion.

Together with the results provided in Section 3.5, which demonstrated that the tested calcium compounds—i.e., $Ca(acac)_2$, $Ca(OAc)_2$, $Ca(OH)_2$, and $CaCO_3$—had a high suppression ability, the results described in this section imply that the four calcium compounds exhibit a flame inhibition effects in the gas phase but not in the condensed phase.

5. Relationship between total bond energy and flame inhibition efficiency

As explained above, the flame-inhibition experiments and TG measurements led us to conclude

that the four calcium compounds investigated in this study possess combustion inhibition ability solely in the gas phase. Thus, we expect that compounds that readily release atomic calcium are efficient combustion inhibitors. In other words, MEC is positively correlated with the bond energy (E_b) of calcium and its counterions in each compound.

To verify this hypothesis, for the four calcium compounds, namely, $Ca(acac)_2$, $Ca(OAc)_2$, $Ca(OH)_2$, and $CaCO_3$, the C_E variation as a function of the total bond energy, which is the enthalpy required to break all the bonds between the calcium and its counterions, is plotted in Fig. 9. The total bond energies for $Ca(OAc)_2$, $CaCO_3$, and $Ca(acac)_2$ are determined from thermodynamic databases, whereas the energy value for $Ca(OH)_2$ is calculated using the couple-cluster theory (CCSD(T) level) with the awCVnZ (n = T, core-valence) basis set [37–40]. We note that the bond-energy values were determined at 25 °C for the sake of simplicity. The data points undoubtedly lie on a straight line with a high coefficient of determination (R^2 = 0.99). Furthermore, the calcium compounds with nearly the same total bond-energy values, namely $Ca(acac)_2$ and $Ca(OAc)_2$, exhibited almost the same C_E values. This result clearly suggests a positive correlation between the ease with which the compounds release calcium and their flame inhibition efficiency.

By definition, the decomposition temperature is the temperature at which a substance begins to chemically decompose. In other words, at the decomposition temperature, the substance is not always necessarily broken down entirely into its atomic species. On the basis of the findings of Cotton et al.

[10], who stated that the free atomic metal species shown in Fig. 4 act as key species in the calcium-catalyzed radical recombination reactions, we assumed the formation of free atomic calcium. As described earlier, the relationship shown in Fig. 9 is highly linear, which also provides concrete evidence that the assumption is not faulty.

Inert chemical species (i.e., carbon dioxide and water) that were produced from $CaCO_3$ and $Ca(OH)_2$ also inhibit flames, and the positive enthalpy change (i.e., endothermic reaction) also has a positive effect on fire suppression. However, as depicted in Fig. 9, a highly linear relationship between the bond energy and the flame inhibition efficiency was observed. This linearity clearly implies that the flame-inhibition efficiency of the calcium species far surpassed that of the such inert species and enthalpies.

The current work clearly demonstrated that the calcium compounds we tested should act as excellent flame inhibitors and the above-mentioned results provide useful insights into the molecular design and development of a novel calcium-based fire-extinguishing agent.

6. Conclusions

To develop a phosphorus-free fire suppressant, the present study experimentally investigated the flame inhibition efficiency of calcium compounds, namely $Ca(acac)_2$, $Ca(OAc)_2$, $Ca(OH)_2$, $CaCO_3$,

$Ca(NO_3)_2$, and CaO, by measuring the downward flame spread rates over thermally thin cellulosic fuels on which each calcium compound was adsorbed. Furthermore, the kinetic parameters (i.e., activation energy and pre-exponential factor associated with the pyrolysis of cellulose) and char yields were determined using a TG analyzer.

As a consequence, the fire-suppression tests involving filter-paper combustion demonstrated that among the calcium compounds tested, $Ca(acac)_2$, $Ca(OAc)_2$, $Ca(OH)_2$, and $CaCO_3$ can completely extinguish flames.

The fire-suppression trials also provided C_E values of 0.36×10^{-3} and 0.31×10^{-3} mol g^{-1}, which clearly indicate that $Ca(acac)_2$ and $Ca(OAc)_2$ have a higher flame inhibition ability by factors of approximately 1.4 and 1.6, respectively, than ADP, which is a conventional phosphate-based fire-extinguishing agent.

The kinetic approach via TG measurements revealed no significant differences in terms of activation energy, pre-exponential factors, and char yields associated with the pyrolysis/combustion of cellulose between the pure cellulose and cellulose mixed with calcium compounds—i.e., $Ca(acac)_2$, $Ca(OAc)_2$, $Ca(OH)_2$, and $CaCO_3$. This result clearly indicates that the calcium compounds do not affect the cellulose pyrolysis and combustion when in solid form. Taken together, the results obtained from the fire-suppression experiments and TG measurements indicate that the calcium compounds acted as flame inhibitors solely in the gas phase.

Plots of the total bond energy and C_E were obviously linear (R^2 = 0.99), thus implying a positive relationship between the ease with which the calcium compounds break down and the combustion-inhibition capability.

In conclusion, the calcium compounds examined in this study will serve as promising flame inhibitors. Furthermore, the key findings of this research lay the groundwork for the design and development of a new, high-performance, phosphorus-free calcium-based fire suppressant that would makes a significant contribution to reducing casualties due to fires and the conservation of limited phosphorus resources.

Conflict of interest

The authors declare no conflicts of interest.

Funding

YK gratefully acknowledges the financial supports from the Limestone Association of Japan and Japan Society for the Promotion of Science (KAKENHI, Grant number: JP19H02387).

Acknowledgments

The FE-SEM observations were performed at the Instrumental Analysis Center of Yokohama National University.

References

1. D. Cordell, J.O. Drangert, S. White, The story of phosphorus: global food security and food for thought, Glob. Env. Change 19 (2009) 292–305. https://doi.org/10.1016/j.gloenvcha.2008.10.009.
2. U.S. Geological Survey, Phosphate rock statistics. https://www.usgs.gov/, 2017 (accessed 5 March 2019).
3. L. Cisse, T. Mrabet, World phosphate production: overview and prospects, Phosphorus Res. Bull. 15 (2004) 21–25. https://doi.org/10.3363/prb1992.15.0_21.
4. X. Ni, K. Kuang, D. Yang, X. Jin, G. Liao, A new type of fire suppressant powder of $NaHCO_3$/zeolite nanocomposites with core–shell structure, Fire Saf. J. 44 (2009) 968–975. https://doi.org/10.1016/j.firesaf.2009.06.004.
5. Y. Koshiba, K. Iida, H. Ohtani, Fire extinguishing properties of novel ferrocene/surfynol 465 dispersions, Fire Saf. J. 72 (2015) 1–6. http://dx.doi.org/10.1016/j.firesaf.2015.02.011.
6. Y. Koshiba, S. Okazaki, H. Ohtani, Experimental investigation of the fire extinguishing capability of ferrocene-containing water mist, Fire Saf. J. 83 (2016) 90–98. http://dx.doi.org/10.1016/j.firesaf.2016.05.006.

7. X. Ni, X. Wang, S. Zhang, M. Zhao, Experimental study on the performance of transition metal ions modified zeolite particles in suppressing methane/air coflowing flame on cup burner, J. Fire Sci. 32 (2014) 417–430. https://doi.org/10.1177/0734904114529402.

8. Y. Koshiba, Y. Takahashi, H. Ohtani, Flame suppression ability of metallocenes (nickelocene, cobaltocene, ferrocene, manganocene, and chromocene), Fire Saf. J. 51 (2012) 10–17. http://dx.doi.org/10.1016/j.firesaf.2012.02.008.

9. M. Chen, D. Zhao, Y. Liu, F. Li, S. Li, Study on preparation and extinguishing fire ability of $KHCO_3/\gamma\text{-}Al_2O_3$ composites, Chem. Lett. 44 (2015) 1552–1554. https://doi.org/10.1246/cl.150742.

10. D.H. Cotton, D.R. Jenkins, Catalysis of radical-recombination reactions in flames by alkaline earth metals, Trans. Faraday Soc. 67 (1971) 730–739. https://doi.org/10.1039/TF9716700730.

11. R. Zalosh, Metal hydride fires and fire suppression agents, J. Loss Prev. Process Ind. 21 (2008) 214–221. https://doi.org/10.1016/j.jlp.2007.06.014.

12. C. Fluegeman, T. Hilton, K.P. Moder, R. Stankovich, Development of detailed action plans in the event of a sodium hydride spill/fire, Process Saf. Prog. 24 (2005) 86–90. https://doi.org/10.1002/prs.10064.

13. A. Hamins, Flame extinction by sodium bicarbonate powder in a cup burner, Symp. (Int.) Combust. 27 (1998) 2857–2864. https://doi.org/10.1016/S0082-0784(98)80144-6.

14. JIS P3801, Filter paper for chemical analysis, in: JIS Handbook, Tokyo, 2015.

15. L.K. Honda, P.D. Ronney, Effect of ambient atmosphere on flame spread at microgravity, Combust. Sci. Technol. 133 (1998) 267–291. https://doi.org/10.1080/00102209808952037.

16. P.D. Ronney, J.B. Greenberg, Y. Zhang, V. Roegner, Flame spread over thin solid fuels in partially premixed atmospheres, Combust Flame. 100 (1995) 474–484. https://doi.org/10.1016/0010-2180(94)00132-C.

17. S. Bhattacharjee, C. Paolini, W. Tran, J.R. Villaraza, S. Takahashi, Temperature and CO_2 fields of a downward spreading flame over thin cellulose: a comparison of experimental and computational results, Proc. Combust. Inst. 35 (2015) 2665–2672. https://doi.org/10.1016/j.proci.2014.05.093.

18. J.N. de Ris, Spread of a laminar diffusion flame, Symp. (Int.) Combust. 12 (1969) 241–252. https://doi.org/10.1016/S0082-0784(69)80407-8.

19. Society of Fire Protection Engineers, SFPE handbook of fire protection engineering, in: Quintiere JG (Ed.), Surface flame spread, third ed., Massachusetts, 2002, pp. 2-246–2-257.

20. D. Drysdale, An introduction to fire dynamics, third ed., Wiley, West Sussex, 2011, pp. 284–307.

21. S. Bhattacharjee, M. Bundy, C. Paolini, G. Patel, W. Tran, A novel apparatus for flame spread study, Proc. Combust. Inst. 34 (2013) 2513–2521. https://doi.org/10.1016/j.proci.2012.05.076.

22. Y. Koshiba, S. Agata, T. Takahashi, H. Ohtani, Direct comparison of the flame inhibition efficiency of transition metals using metallocenes, Fire Saf. J. 73 (2015) 48–54.

http://dx.doi.org/10.1016/j.firesaf.2015.03.003.

23. H. Feilchenfeld, Z.E. Jolles, D. Meisel, The effect of bromides on the burning properties of polyester, Combust. Flame 15 (1970) 247–254. https://doi.org/10.1016/0010-2180(70)90004-0.

24. R.J. McCarter, Combustion inhibition of cellulose by powders: Preliminary data and hypotheses, Fire Mater. 5 (1981) 66–72. https://doi.org/10.1002/fam.810050206.

25. M. Izumikawa, T. Mitani, T. Niioka, Flame spread of paper sheets containing suppressants, Trans. Jpn. Soc. Mech. Eng. B 52 (1986) 1413–1419 (in Japanese). https://doi.org/10.1299/kikaib.52.1413.

26. T. Hirano, K. Saito, Fire spread phenomena: the role of observation in experiment, Prog. Ener. Combust. Sci. 20 (1994) 461–485. https://doi.org/10.1016/0360-1285(94)90001-9.

27. Society of Fire Protection Engineers, SFPE handbook of fire protection engineering, in: Beyler CL, Hirschler MM (Eds.), Thermal decomposition of polymers, third ed., Massachusetts, 2002, pp. 1-110–1-131.

28. I.K. Henderson, R. Saari-Nordhaus, Analysis of commercial explosives by single-column on chromatography, J. Chromatogr. 602 (1992) 149–154. https://doi.org/10.1016/0021-9673(92)80075-6.

29. K. Cheng, W.T. Winter, A.J. Stipanovic, A modulated-TGA approach to the kinetics of lignocellulosic biomass pyrolysis/combustion, Polym. Degrad. Stabil. 97 (2012) 1606–1615.

https://doi.org/10.1016/j.polymdegradstab.2012.06.027.

30. U.-J. Kim, S.H. Eom, M. Wada, Thermal decomposition of native cellulose: influence on crystallite size, Polym. Degrad. Stabil. 95 (2010) 778–781. https://doi.org/10.1016/j.polymdegradstab.2010.02.009.

31. P. Paik, K.K. Kar, Kinetics of thermal degradation and estimation of lifetime for polypropylene particles: Effects of particle size, Polym. Degrad. Stabil. 93 (2008) 24–35. https://doi.org/10.1016/j.polymdegradstab.2007.11.001.

32. R.L. Blaine, H.E. Kissinger, Homer Kissinger and the Kissinger equation, Thermochim. Acta 540 (2012) 1–6. http://dx.doi.org/10.1016/j.tca.2012.04.008.

33. F. Richter, G. Rein, Pyrolysis kinetics and multi-objective inverse modelling of cellulose at the microscale, Fire Saf. J. 91 (2017) 191–199. https://doi.org/10.1016/j.firesaf.2017.03.082.

34. D. Shen, J. Ye, R. Xiao, H. Zhang, TG-MS analysis for thermal decomposition of cellulose under different atmospheres, Carbohydr. Polym. 98 (2013) 514–521. https://doi.org/10.1016/j.carbpol.2013.06.031.

35. M. Amutio, G. Lopez, R. Aguado, M. Artetxe, J. Bilbao, M. Olazar, Kinetic study of lignocellulosic biomass oxidative pyrolysis, Fuel 95 (2012) 305–311. https://doi.org/10.1016/j.fuel.2011.10.008.

36. A.W. Musumeci, R.L. Frost, E.R. Waclawik, A spectroscopic study of the mineral paceite (calcium

acetate), Spectrochim. Acta A 67 (2007) 649–661. https://doi.org/10.1016/j.saa.2006.07.045.

37. S. Thakur, Calorimetric studies of the acetates of calcium (II), strontium (II) and barium (II), Asian J. Chem. 20 (2008) 1645–1647.

38. M. Vasiliu, D. Feller, J.L. Gole, D.A. Dixon, Structures and heats of formation of simple alkaline earth metal compounds: fluorides, chlorides, oxides, and hydroxides for Be, Mg, and Ca, J. Phys. Chem. A 114 (2010) 9349–9358. https://doi.org/10.1021/jp1050657.

39. H.D.B. Jenkins, K.F. Pratt, B.T. Smith, T.C. Waddington, Lattice potential energies for calcite, aragonite and vaterite: estimation of the charge distribution on the carbonate ion, the enthalpy of formation, $\Delta H_f^\circ(CO_3^{2-})$ (g) and the enthalpy of solvation, $\Delta H_{solv}^\circ(CO_3^{2-})$ (g) of the gaseous CO_3^{2-} ion, J. Inorg. Nucl. Chem. 38 (1976) 371–377. https://doi.org/10.1016/0022-1902(76)80265-5.

40. M.A.V. Ribeiro da Silva, M.LC.C.H. Ferrao, Energetics of metal-oxygen bonds in metal complexes of β-diketones, Pure Appl. Chem. 60 (1988) 1225–1234. https://doi.org/10.1351/pac198860081225.

Table captions

Table 1

Observed minimum extinction concentrations (MEC, C_E) of the investigated calcium compounds. A smaller C_E value corresponds to a more effective inhibiting of flames. The C_E values are determined from Figure 6.

Table 2

Temperature at which the weight-loss rates are maximum, T_{max}, in the TG measurements of the specimens.

Table 3

Activation energies and natural logarithms of the pre-exponential factors of the specimens determined by the Kissinger method—Eq. (10).

Table 4

Char yields determined by TG measurements of the specimens. A greater *Y* value corresponds to a more effective hampering of char combustion by the inhibitor.

Figure captions

Fig. 1

Chemical structure of $Ca(acac)_2$. In this figure, Me represents the methyl group.

Fig. 2

Experimental procedures for preparing the rectangular paper specimens on which each calcium compounds was adsorbed.

Fig. 3

Schematic of the experimental apparatus for determining the downward flame spread rates.

Fig. 4

Major radical recombination pathways for the calcium species [10]. X represents the third body.

Fig. 5

Schematic of the downward flame spread over a thin solid fuel. U, δ, and g denote the downward flame spread rate, solid-fuel thickness, and acceleration due to gravity, respectively.

Fig. 6

Normalized flame-spread rate V as a function of the concentration of (a) ADP, (b) CaO, (c) $Ca(NO_3)_2$, (d) $CaCO_3$, (e) $Ca(OH)_2$, (f) $Ca(acac)_2$, and (g) $Ca(OAc)_2$.

Fig. 7

TG and DTG curves at a heating rate of 10 K min^{-1} under a nitrogen atmosphere. (a) Pure cellulose, (b) $Ca(acac)_2$/cellulose, (c) $Ca(OAc)_2$/cellulose, (d) $Ca(OH)_2$/cellulose, (e) $CaCO_3$/cellulose, (f) pure $Ca(acac)_2$, and (g) pure $Ca(OAc)_2$. Note that the x axes indicate the concentrations of compound k on the rectangular paper specimens, C_k.

Fig. 8

Variations in $\ln(\beta\ T_{max}^{-2})$ as a function of T_{max}^{-1} of the specimens. (a) $Ca(acac)_2$/cellulose, (b) $Ca(OAc)_2$/cellulose, (c) $Ca(OH)_2$/cellulose, and (d) $CaCO_3$/cellulose. β and T_{max} denote the heating rate and temperature where the weight loss rate is maximized, respectively.

Fig. 9

Total bond energy as a function of C_E. Note that the bond-energy data for $Ca(OAc)_2$, $Ca(OH)_2$, $CaCO_3$, and $Ca(acac)_2$ were adapted from the works of Thakur [37], Vasilu et al. [38], Jenkins et al. [39], and Ribeiro da Silva and Ferrao [40], respectively.

Figure 1

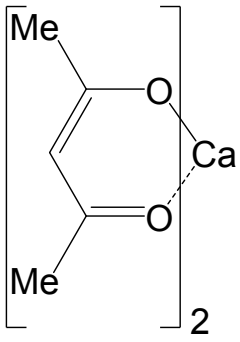

Figure 2

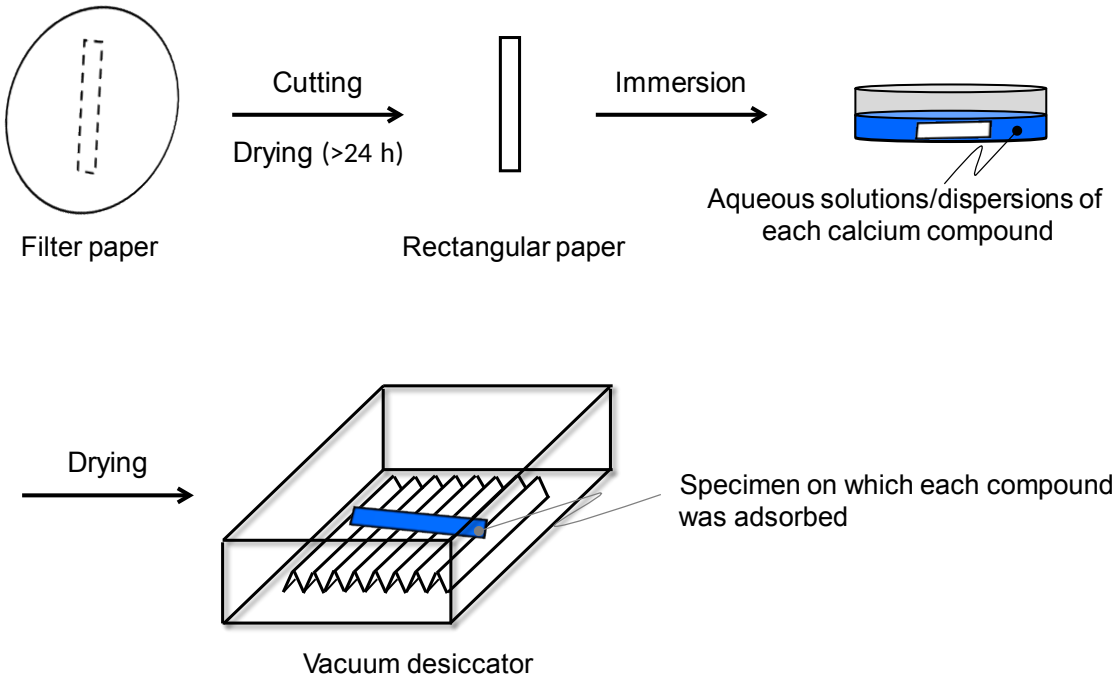
Cutting
Drying (>24 h)
Immersion
Filter paper
Rectangular paper
Aqueous solutions/dispersions of each calcium compound
Drying
Specimen on which each compound was adsorbed
Vacuum desiccator

Figure 3

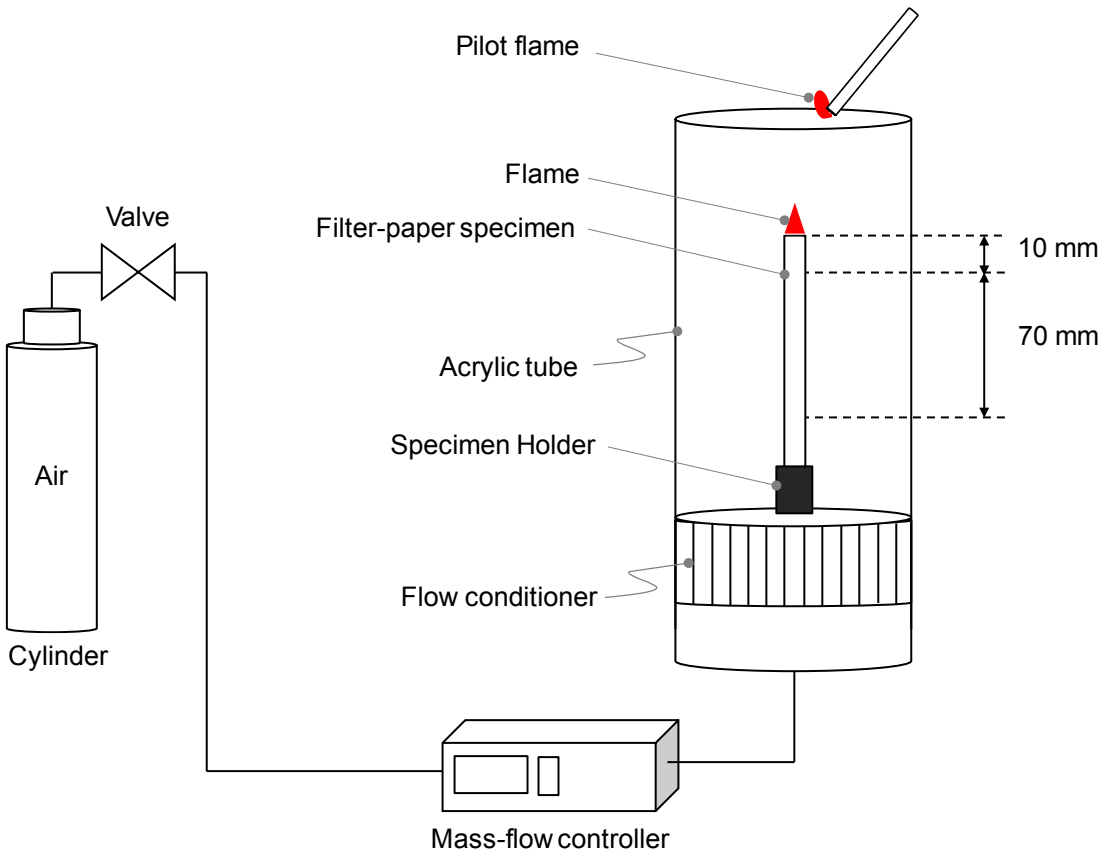
Pilot flame
Flame
Filter-paper specimen
10 mm
70 mm
Valve
Acrylic tube
Specimen Holder
Air
Flow conditioner
Cylinder
Mass-flow controller

Figure 4

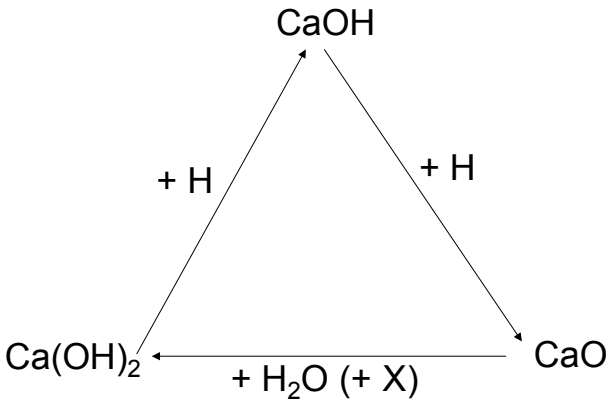

Figure 5

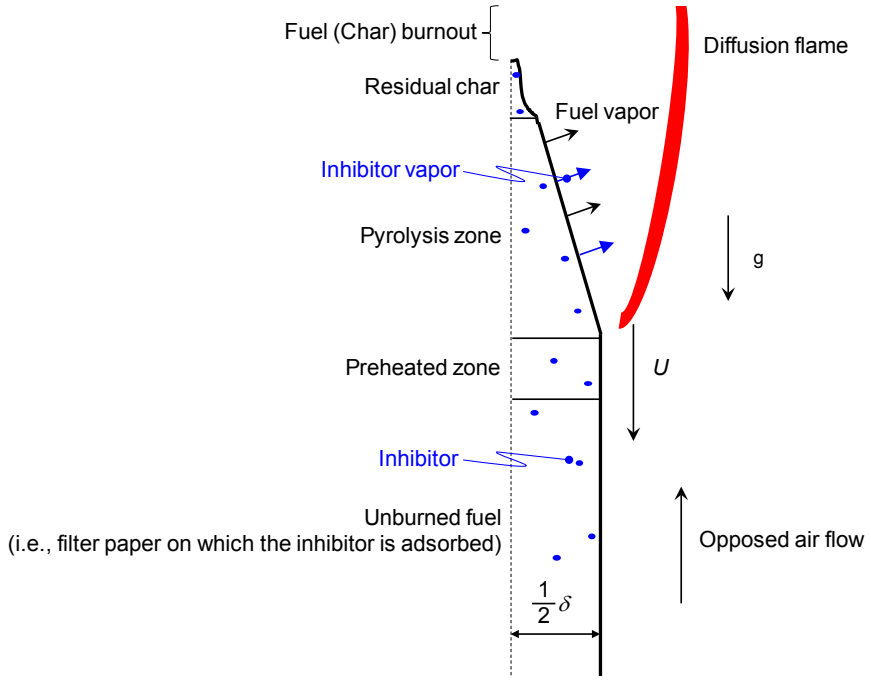
Fuel (Char) burnout
Residual char
Fuel vapor
Diffusion flame
Inhibitor vapor
Pyrolysis zone
g
Preheated zone
U
Inhibitor
Unburned fuel
(i.e., filter paper on which the inhibitor is adsorbed)
Opposed air flow
$\frac{1}{2}\delta$

Figure 6

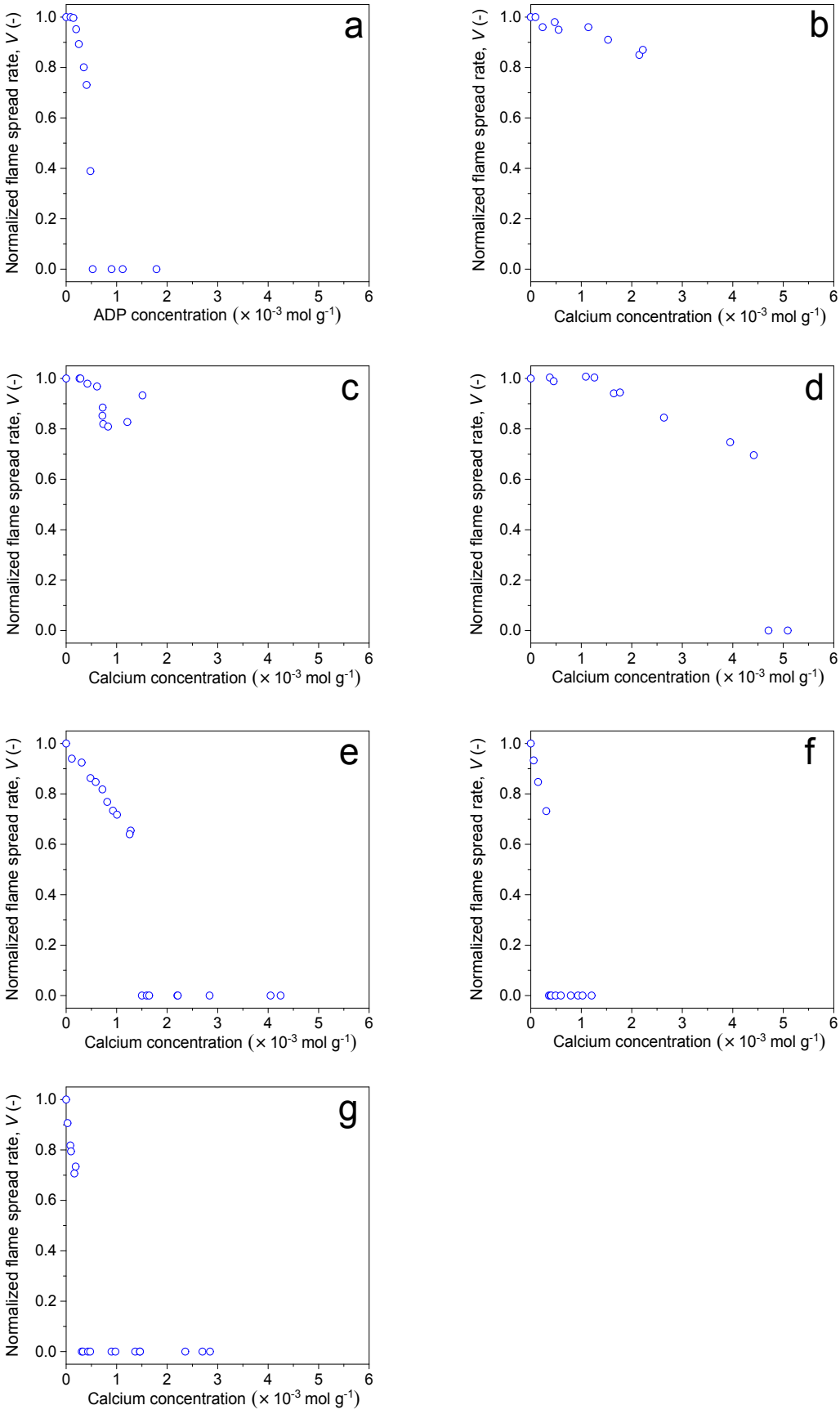
a
Normalized flame spread rate, V (-)
ADP concentration (× 10-3 mol g-1)
b
Normalized flame spread rate, V (-)
Calcium concentration (× 10-3 mol g-1)
c
Normalized flame spread rate, V (-)
Calcium concentration (× 10-3 mol g-1)
d
Normalized flame spread rate, V (-)
Calcium concentration (× 10-3 mol g-1)
e
Normalized flame spread rate, V (-)
Calcium concentration (× 10-3 mol g-1)
f
Normalized flame spread rate, V (-)
Calcium concentration (× 10-3 mol g-1)
g
Normalized flame spread rate, V (-)
Calcium concentration (× 10-3 mol g-1)

Figure 7

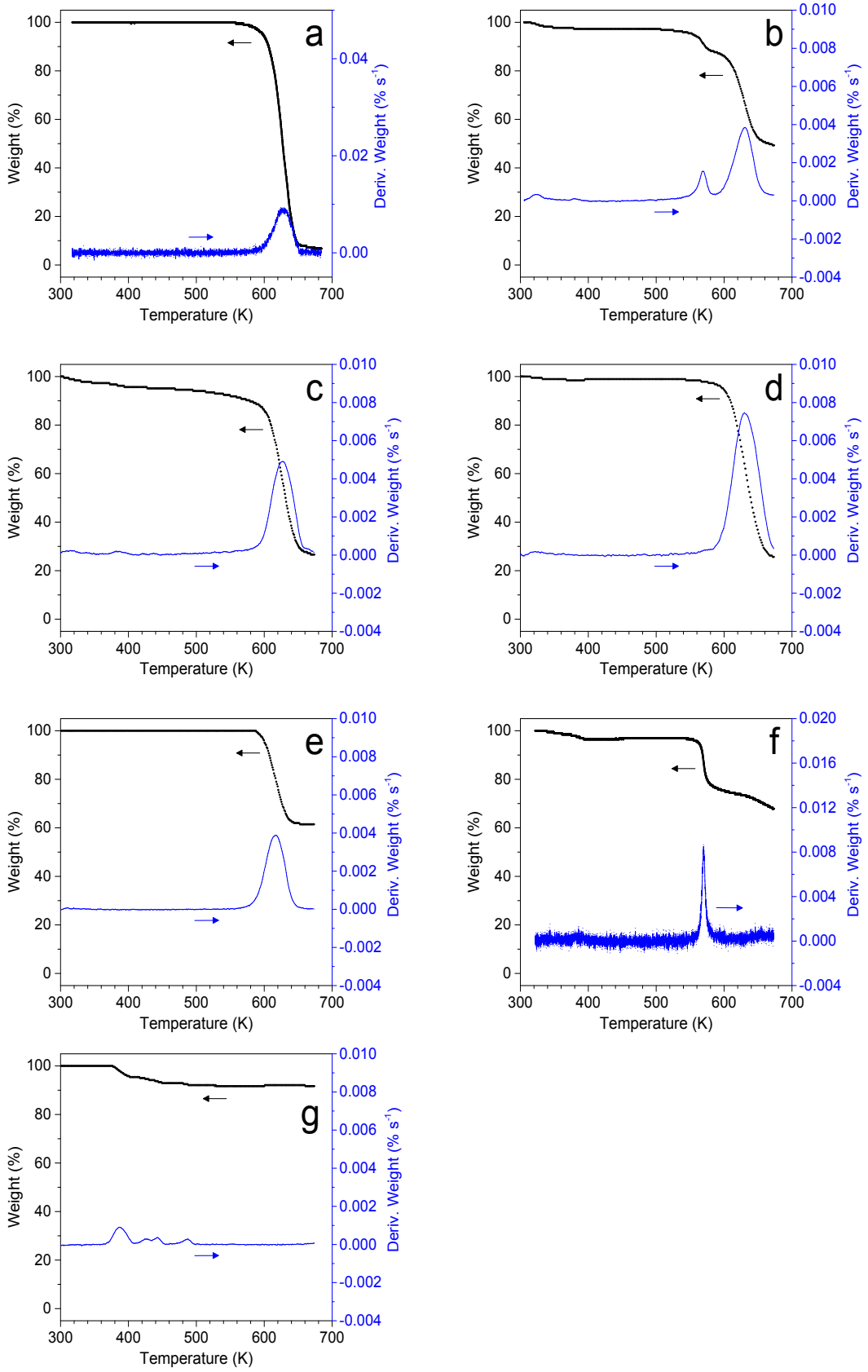

Figure 8

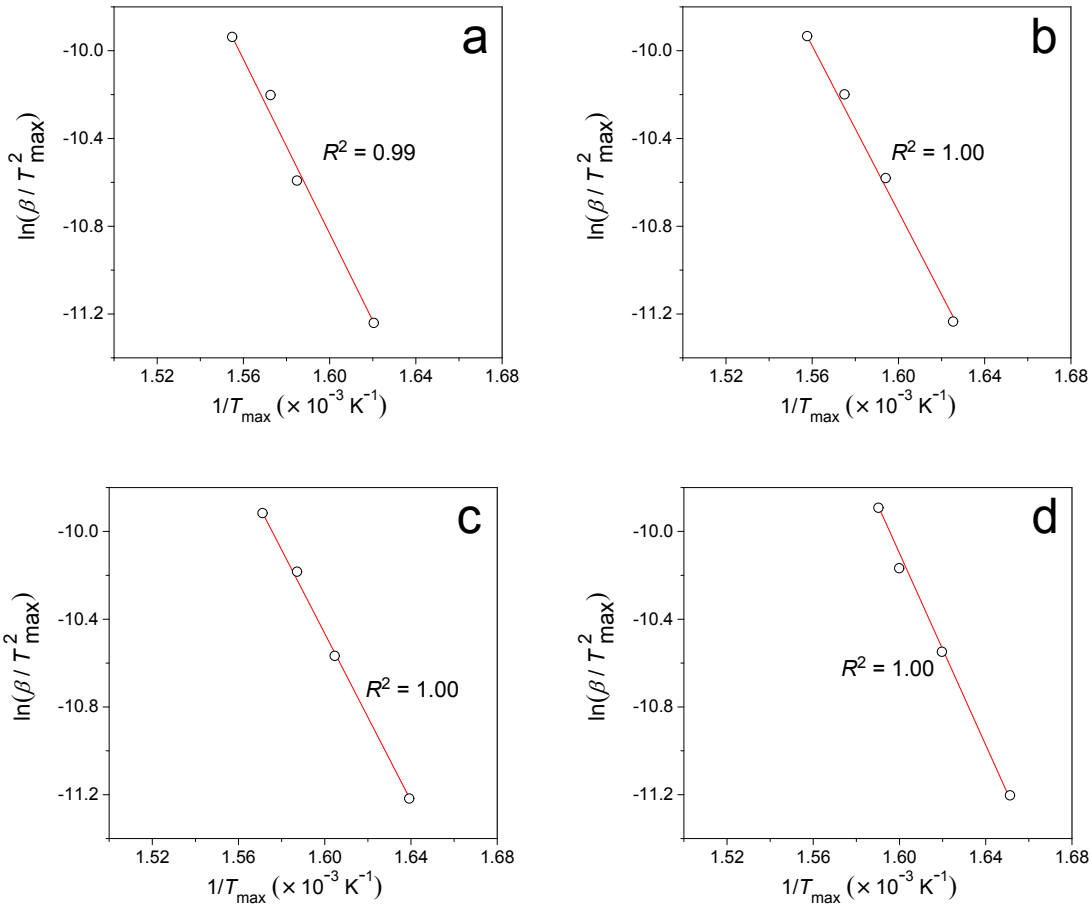
a
b
c
d
R^2 = 0.99
R^2 = 1.00
R^2 = 1.00
R^2 = 1.00
$\ln(\beta / T^2_{max})$
$1/T_{max}$ ($\times 10^{-3}$ K^{-1})
-10.0
-10.4
-10.8
-11.2
1.52
1.56
1.60
1.64
1.68

Figure 9

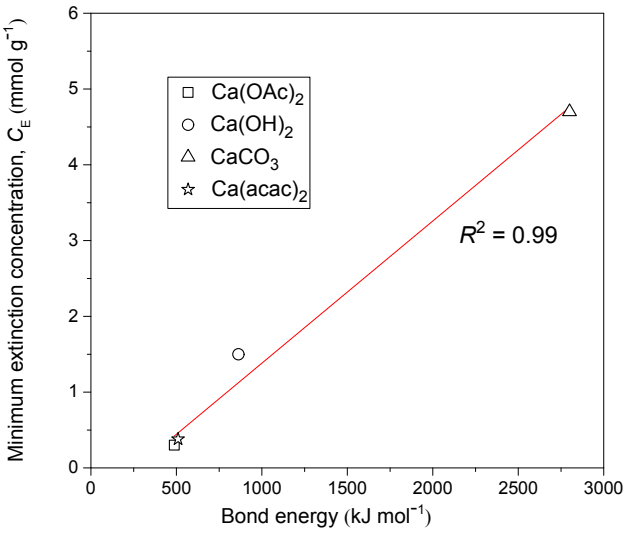
Minimum extinction concentration, C_E (mmol g^{-1})
Bond energy (kJ mol^{-1})
Ca(OAc)$_2$
Ca(OH)$_2$
CaCO$_3$
Ca(acac)$_2$
R^2 = 0.99
0
1
2
3
4
5
6
0
500
1000
1500
2000
2500
3000

Table 1

Compound	Minimum extinction concentration, C_E (mol g^{-1})
Calcium carbonate ($CaCO_3$)	4.71×10^{-3}
Calcium hydroxide ($Ca(OH)_2$)	1.50×10^{-3}
Calcium acetylacetonate ($Ca(acac)_2$)	0.36×10^{-3}
Calcium acetate ($Ca(OAc)_2$)	0.31×10^{-3}
ADP ($NH_4H_2PO_4$) [a]	0.53×10^{-3}

a: adapted from Ref. [8].

Table 2

Specimen [a]	T_{max} (K)
$Ca(acac)_2$/cellulose	643
$Ca(OAc)_2$/cellulose	642
$Ca(OH)_2$/cellulose	636
$CaCO_3$/cellulose	629
Pure cellulose	629

a: The concentration of each calcium compound is the MEC value (see Table 1).

Note: T_{max} represents the temperature at which the weight-loss rate was maximized.

Table 3

Calcium compound	E (kJ mol^{-1})	ln$A$	R^2
$Ca(acac)_2$/cellulose	169	33.0	0.99
$Ca(OAc)_2$/cellulose	162	30.3	1.00
$Ca(OH)_2$/cellulose	161	30.4	1.00
$CaCO_3$/cellulose	175	33.5	1.00
Pure cellulose	171	32.6	1.00

Note: E, A, and R^2 denote the activation energy, pre-exponential factor, and coefficient of determination, respectively.

Table 4

Specimen	Char yield, Y (%)
$Ca(acac)_2$/cellulose	0.5
$Ca(OAc)_2$/cellulose	0.1
$Ca(OH)_2$/cellulose	4.8
$CaCO_3$/cellulose	0.6
Pure cellulose	0.0

Note: Char yields were determined at 873 K.

Conflict of interest

None of authors have any conflicts of interest to declare.